

# The use of solid residues derived from different industrial activities to obtain calcium silicates for use as insulating construction materials

M. Felipe-Sesé, D. Eliche-Quesada, F.A. Corpas-Iglesias \*

*Departamento de Ingeniería Química, Ambiental y de los Materiales, EPS de Linares, Universidad de Jaén, 23700 Linares (Jaén), Spain*

Received 4 March 2011; received in revised form 29 April 2011; accepted 2 May 2011

Available online 10 May 2011

## Abstract

Calcium silicates have obtained through solid state reaction of the different residues generated in various industrial activities. As a source of calcium oxide: marble, mussel shells, and the reagent commercial calcium hydroxide were used. The source of silica was biomass ash and fired ceramic residue formed by crushing pieces of broken and defective ceramic products from a brick factory (chamotte). From the raw materials, biomass ash and marble, biomass ash and commercial calcium hydroxide, and chamotte and crushed mussel shell dust, mixed in a molar ratio  $\text{CaO}:\text{SiO}_2$  1:1 and sintered at 1100 °C (24 h), calcium silicates such as wollastonite, gehlenite and larnite were obtained. Both the raw materials and the synthesized material were characterized by XRD, XRF and TGA–DTA. In order to use the calcium silicates obtained as low temperature thermal insulating ceramic materials, the materials obtained were compressed under uniaxial loading at 81.7 MPa to obtain bricks measuring 60 mm × 30 mm × 10 mm. The properties of the bricks were studied. The ceramic materials present conductivity values between 0.10 W/m<sup>2</sup> K and 0.18 W/m<sup>2</sup> K and compressive strength of 29.8–59.3 MPa, respectively. The bricks met the UNE guidelines for use as low-temperature structural insulation ceramics.

© 2011 Elsevier Ltd and Techna Group S.r.l. All rights reserved.

**Keywords:** Calcium silicates; Construction materials; Residues; Recycling

## 1. Introduction

There is a direct relationship between a country's degree of development as represented by its citizens' per capita income and the generation of large quantities of solid residues. The richer a country is, the more its residues increase. If we are to prevent the collapse of the means of production and of the plants, we cannot continue the current rate at which we generate residues. We must reduce them by fostering reuse and recycling [1–5].

The Spanish ceramics sector is the largest European producer of construction bricks. Entrepreneurial activity of the ceramics industry extends throughout the national territory, and the region of Andalusia is the second largest producer of bricks and tiles, after Castilla-La Mancha. The city of Bailén (Jaén) is the main centre of production in Andalusia [6]. This industry generates residues of fired products from partially

broken or defective and thus unsellable materials (chamotte). At present, their use before grinding is very widespread in all of the ceramics sectors, both the brick and tile production industry and sanitary ware, depending on the amount of the product that can be reintroduced [7–10]. This material is also being used as a degreasing agent and as a raw material for making Portland cement clinker [11]. Its use is not profitable, however, since special grinding installations are needed to grind the fired materials, with significant additional maintenance costs that do not usually compensate for the savings on raw materials, hence the current problem.

In the wooden board manufacturing industry, the residues generated during processing (constituted primarily of wood scraps from the bark of conifers) are used as fuel to obtain electrical and thermal energy. The combustion process generates a large quantity of ashes as residue, which usually accumulates in authorized dumps. Both the ashes and the chamotte are potential sources of oxides, primarily silica.

The marble industry generates residues from the accumulation of large quantities of dust and white mud during the process of cutting and polishing the material. The materials are

\* Corresponding author. Tel.: +34 953648565.

E-mail address: [facorpas@ujaen.es](mailto:facorpas@ujaen.es) (F.A. Corpas-Iglesias).

constituted mainly of calcium carbonate. To illustrate the magnitude of the waste, sawing 3000 m<sup>2</sup> of marble alone generates 600 tonnes of residue. Broadly speaking, environmental problems in the marble sector consist of the dumping of residues and mud from the processing industry into public waterways, as well as the serious degradation of the urban environment in population centres that house the industries.

The canning industry is one of the most important industries in the north of Spain, especially in Galicia, and particularly in the conservation of mussels. After China, Galicia is the first world producer of mussels. Every year, the mussel sector produces 256,000 tonnes of mussels, of which 65% is processed by the canning and freezing sector, producing 81,000 tonnes of mussel shell residue. The canneries, boileries, and refineries have great difficulty getting rid of the mussel shells after processing and packaging the mussels. Mussel shell is not a toxic or dangerous residue. The biggest problem is the smell emitted by the decomposing organic material, which enables the shell to be colonized by microorganisms, among them pathogens that can be transmitted to humans or animals. The accumulation of the shells also creates visually unattractive mountains of residue with serious drawbacks from the perspective of the environment, landscape, and even economics. One possible solution to this problem is to deposit the mussel shells in authorized dumps, although this causes problems as well. Both marble residue and mussel shells are composed primarily of calcium carbonate.

Calcium silicates are composed of the system CaO–SiO<sub>2</sub>, including wollastonite, which is generated in nature mainly by hydrothermal processes of mixing limestone sediments with silica [12,13]. Other interesting composites are dicalcium and tricalcium silicate, which are important phases in cement. The most important applications of calcium silicates are found in the ceramics industry, in manufacturing tough ceramics and bioceramics, in metal foundries as melting additives or simply as loads or coating, in the manufacturing of dielectric porcelains, in paints, in the composition of bioactive glass, in the production of resins and plastics (polyester, polyvinyl, nylon or polypropylene), and as a reinforcement material to improve the physical, chemical and electrical properties of the finished product. They are also used in the production of insulating ceramic as a substitute for bones and coatings [14–18].

Building on these antecedents, the present study used ashes and chamotte as a source of silica, the residue from marble remains and mussel shells, and the reagent commercial calcium hydroxide as a source of calcium oxide from which to obtain calcium silicates. Further, the bricks were formed by uniaxial compression of the silicates obtained. We studied their technological properties to determine their application as low-temperature thermal insulating ceramic materials.

## 2. Materials and methods

### 2.1. Preparation of the samples

The different calcium silicates were synthesized using different residues. As a source of silica, ash from the combustion

of by-products from the processing of boards was used. The wood was generated by installations in the factory Tableros Tradema S.L., located in the city of Linares (Jaén) (Spain). We also used scraps of broken or defective brick (chamotte) from the installations of a factory that manufactures hollow ceramic bricks located in Bailén (Jaén) (Spain). As a source of calcium oxide, two residues were used: the dust from cutting and polishing the marble originating from the installations of the firm Triturados Blanco Macael S.A., located in Macael (Almería) (Spain) and mussel shells from the conservation processes and the commercial reagent calcium hydroxide.

The biomass ash has a heterogeneous particle size and includes metal scraps. To eliminate these scraps and the large particles, we sifted the ash with a sieve of mesh size 0.32 mm. Then, part of the ash was introduced into an agate ball mill to obtain a particle size of 100 µm.

The chamotte, marble scraps and mussel shells were ground in a hammer mill and then a ball mill to obtain a particle size of 100 µm.

First, the ground residues were mixed in dry phase in the ball mill for two hours. In the first experiment, biomass ashes and marble and in the second, chamotte and mussel shells were mixed in a molar ratio of SiO<sub>2</sub>:CaO 1:1. In the third experiment, the reaction of the ashes with particle size of 0.32 mm with commercial calcium oxide in aqueous solution at 90 °C for one hour was studied. Both substances were mixed using an agitator and in the same molar ratio CaO:SiO<sub>2</sub> 1:1, using 60 wt% water. Then, the moisture was eliminated by heating the mixture at 110 °C for 24 h. Finally, the three mixes were sintered in a laboratory oven at 1100 °C for 24 h with a heating ramp of 20 °C/min to obtain calcium silicates through solid state reaction.

To study the technological properties and see their application as low-temperature thermally insulating construction materials, the samples were moistened for 20 min with 15 wt% water to make test samples of approximately 60 mm × 30 mm × 10 mm, under uniaxial loading of 81.7 MPa using the laboratory press Mega KCK-30A. After shaping the pieces were dried at 110 °C for 24 h. Finally, the test samples were cured by immersing them in water, 5 min per day for 1 week. The pieces were then dried in an oven at 110 °C for 48 h.

### 2.2. Characterization of the raw materials and synthesized silicates

The X-ray diffraction patterns of the powder obtained from different materials were achieved using a Philips X'Pert Pro automated diffractometer equipped with a Ge (1 1 1) primary monochromator.

Chemical composition of the wastes was determined by X-ray fluorescence (XRF) using the Philips Magix Pro (PW-2440).

The raw materials and sintered silicates were analyzed with thermogravimetric and differential thermal analysis (TGA–DTA) using a Mettler Toledo 851° device in oxygen. The samples were placed in the crucible and heated at a rate of 20 °C/min from room temperature to 1000 °C.

The content of carbonates from the marble, mussel and commercial calcium hydroxide was determined by calcimetry.

CHNS chemical elemental analysis was performed to determine the total amount of carbon, hydrogen, nitrogen and sulphur in the samples using a CHNS-O Thermo Finnigan Elementary Analyzer Flash EA 1112 via combustion in an O<sub>2</sub> atmosphere.

### 2.3. Tests performed on the formed specimen

A series of tests and inspections was performed to determine the physical, mechanical and thermal properties of the bricks.

Bulk density and absolute density were obtained according to standard procedure UNE-EN-772-13 [19].

A test to determine water absorption capacity was implemented according to standard procedure UNE 67027 [20]. The water suction of a brick is the volume of water absorbed during a short partial immersion. The test to determine water suction was implemented according to standard procedure UNE 67-031 [21].

The compressive strength of bricks is bulk unit charge against breakage under axial compressive strength. For this trial, six fired samples were studied. Tests on compressive strength were carried out according to standard UNE-EN 772-1 [22] on a Suzpecar CME 200 SDC laboratory press. Area of both bearing surfaces was measured and the average taken.

All samples were submitted to a progressively increasing normal strength, with the load applied centred on the upper surface of the sample until breakage. The compressive strength of each sample was obtained by dividing the maximum load by the average surface of both bearing surfaces, expressed in MPa with a 0.1 MPa accuracy.

To determine thermal conductivity, a model house of PHYWE high insulation with removable walls and insulated ceiling was used. The material to be tested was placed on one wall. Since steady-state heat flow is constant and the coefficient of heat transfer by convection in the case of closed rooms in the literature is 8.1 W/m<sup>2</sup> K, we can calculate the thermal conductivity of the tested material.

The microstructure of the pieces formed were analyzed using a JEOL SM 840 scanning electron microscope. The samples were placed on an aluminium grate and coated with carbon using an ion sputtering device JEOL JFC 1100.

## 3. Results and discussion

The chemical composition of the crushed marble residue and mussel shell residue after firing at 1100 °C, chamotte and biomass ash was determined by XRF (Table 1). The results indicated that the marble residue contained a significant amount of calcium oxide (55.3%). It also contained smaller amounts of impurities in the form of magnesium, ferrous, silicon and aluminium oxides. The results of XRD and Bernard's calcimetry (98% CaCO<sub>3</sub>) confirmed that this residue contained a large quantity of calcite. The XRD pattern of the marble residue showed a sharp peak corresponding to magnesium calcite (Mg<sub>0.03</sub>Ca<sub>0.97</sub>)(CO<sub>3</sub>) and a less pronounced peak

Table 1  
Chemical composition of wastes.

Oxide content (%)	Biomass ash	Chamotte	Marble	Mussel after firing at 1100 °C
SiO <sub>2</sub>	52.53	59.77	0.93	0.55
Al <sub>2</sub> O <sub>3</sub>	6.88	20.10	0.36	0.03
Fe <sub>2</sub> O <sub>3</sub>	4.92	8.74	0.16	0.05
MnO	0.10	0.08	–	–
MgO	2.62	2.27	1.25	0.49
CaO	14.95	1.73	55.3	87.21
Na <sub>2</sub> O	1.19	0.22	–	0.50
K <sub>2</sub> O	1.96	4.99	–	0.04
TiO <sub>2</sub>	2.59	0.89	–	0.02
P <sub>2</sub> O <sub>5</sub>	0.62	0.14	–	0.09
Zr (ppm)	267.4	1261.5	7.05	–
LoI	11.64	0.67	42.0	–

indicating the presence of dolomite (Ca(Mg(CO<sub>3</sub>)<sub>2</sub>). Traces of quartz were also observed (Fig. 1a). The high loss on ignition (42%) was attributed to the loss of carbon dioxide from the partial dissociation of the calcite and the dolomite.

Like the marble, the inorganic fraction of the mussel shell residue contained a significant quantity of calcium oxide (87.21%). It also contained smaller quantities of impurities, primarily in the form of silicon, sodium and magnesium oxides. The XRD data (Fig. 1b) confirmed that the calcium was found in the form of magnesium calcite (Mg<sub>0.03</sub>Ca<sub>0.97</sub>)(CO<sub>3</sub>) and aragonite. Aragonite is one of the polymorphous crystalline forms of the calcite found in nearly all mussel shells. The carbonate content, primarily calcium carbonate, was 95%. As with the marble residue, the loss on ignition (44.80%) was attributed to the loss of carbon dioxide due to the partial dissociation of both the calcite and the aragonite and combustion of organic matter.

The commercial calcium hydroxide used as a source of calcium was constituted according to its XRD pattern (Fig. 1c) as portlandite (Ca(OH)<sub>2</sub>), which came from moistening the CaO, and as calcite (CaCO<sub>3</sub>), due to carbonation of the CaO.

The residue of the biomass ash was a potential source of oxides. Its most abundant component was SiO<sub>2</sub> (52.53%), but considerable quantities of CaO (15%) and other oxides such as Al<sub>2</sub>O<sub>3</sub>, Fe<sub>2</sub>O<sub>3</sub>, MgO, TiO<sub>2</sub>, K<sub>2</sub>O and Na<sub>2</sub>O that could act as mineralizers were present. The minor components were MnO, P<sub>2</sub>O<sub>5</sub> and ZnO, which were found in smaller quantities of 1%. The loss on ignition was approximately 11% and may be attributed to the loss of volatiles associated with the decomposition of the different composites, including the total organic carbon. The XRD pattern of the ash residue is shown in Fig. 1d. We see the diffraction peaks for aluminium and potassium silicate (K<sub>0.85</sub>Al<sub>0.85</sub>Si<sub>0.15</sub>O<sub>2</sub>), dicalcium silicate (Ca<sub>2</sub>SiO<sub>4</sub>), and minerals such as kalicinite (K(HCO<sub>3</sub>)) and huntite (Mg<sub>3</sub>Ca(CO<sub>3</sub>)<sub>4</sub>). The carbonate content in the ashes was 1.2%.

The chemical composition of the chamotte indicated that it was constituted primarily of silicates and aluminates, with iron, calcium and basic elements (sodium and potassium) present in smaller quantities. The mineralogical composition determined

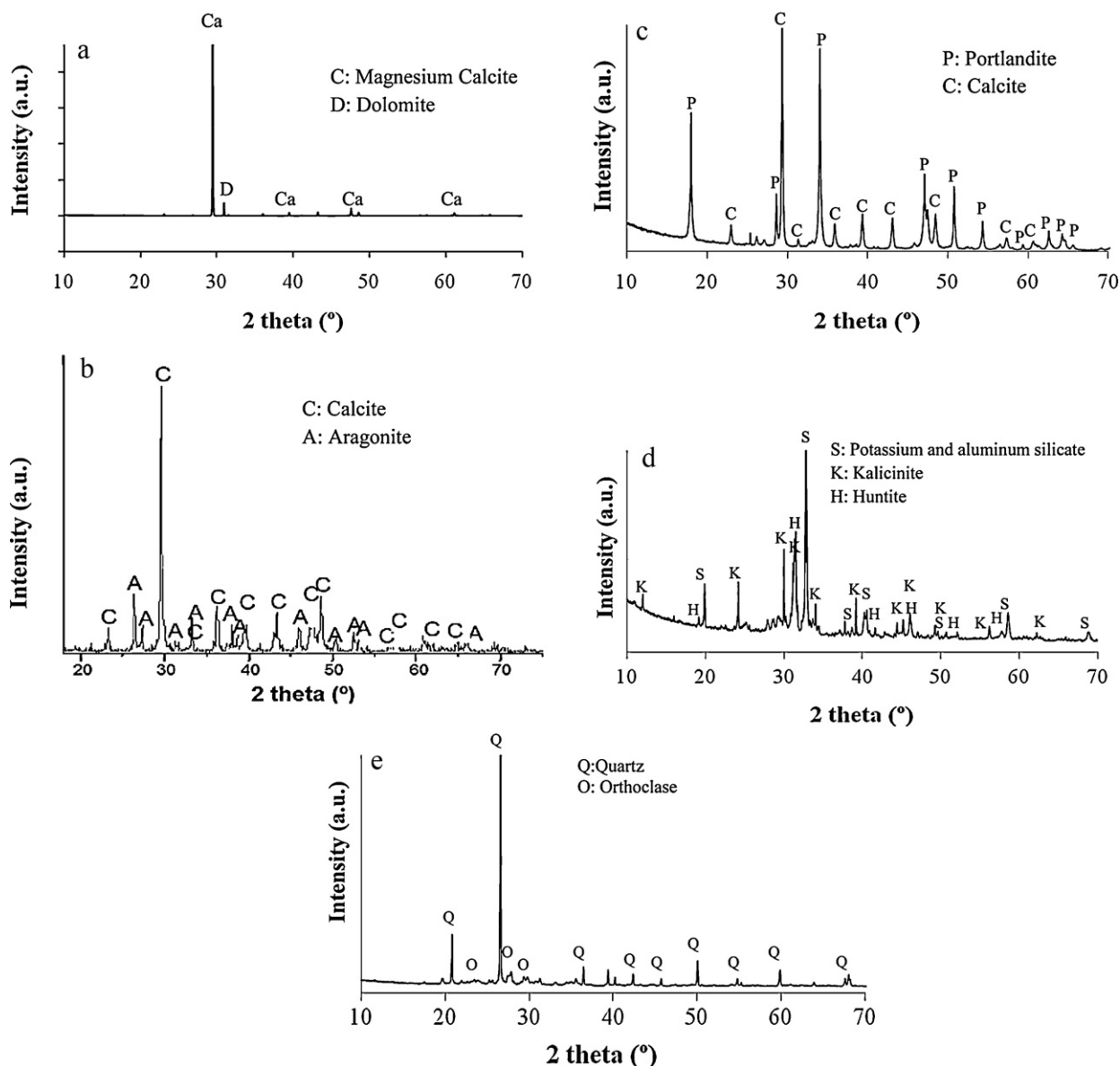


Fig. 1. XRD patterns for powdered (a) marble, (b) mussel, (c) commercial calcium hydroxide, (d) biomass ash, and (e) chamotte.

by XRD (Fig. 1e) indicated that the main crystalline phases in the chamotte were quartz ( $\text{SiO}_2$ ) and small quantities of orthoclase ( $\text{K(Al, Fe) Si}_2\text{O}_8$ ) and albite ( $\text{Na}_{0.98}\text{Ca}_{0.02}\text{Al}_{1.02}\text{Si}_{2.98}\text{O}_8$ ).

For the marble residue, the TGA–DTA graph (Fig. 2a) showed a mass loss of 2.6% from ambient temperature up to 580 °C, due to the loss of moisture, water absorbed and possible water bonded. Between 580 °C and 900 °C, the weight loss of 43% can be associated with the decomposition of the calcium carbonate  $\text{CaCO}_3$  into calcium oxide and  $\text{CO}_2$  with a strong endothermic peak at 830 °C.

In the TGA–DTA curve (Fig. 2b) for the mussel shell residue, a small weight loss of 0.4%, from ambient temperature up to approximately 200 °C, associated with the release of physically absorbed water was observed, showing a small endothermic peak centred around 100 °C. The weight loss of 1.7%, between 200 and 356 °C, was due to oxidation and

removal of the volatile matters of the sample. From 356 °C to 600 °C, a 2.3% weight loss occurred, which may be due to the combustion of organic material, as indicated by the exothermic peaks centred around 345 and 555 °C, as well as the elimination of the possible presence of bonded water, as indicated by the endothermic peak centred around 440 °C. Finally, from 600 °C to 850 °C, there is a much greater mass loss, 43.3%, due to the decomposition of the main component of the mussel shells, calcium carbonate, which appears in the DTA as a strong endothermic peak centred around 827 °C.

In the TGA–DTA analysis of the reagent calcium hydroxide (Fig. 2c), three weight losses was observed. The first small weight loss from ambient temperature up to 125 °C was 0.4%, due to the elimination of the water from moistening, with an endothermic peak centred around 80 °C. The next weight loss up to 518 °C, was much more pronounced, 10.5%. This loss was due to the elimination of structural water from the

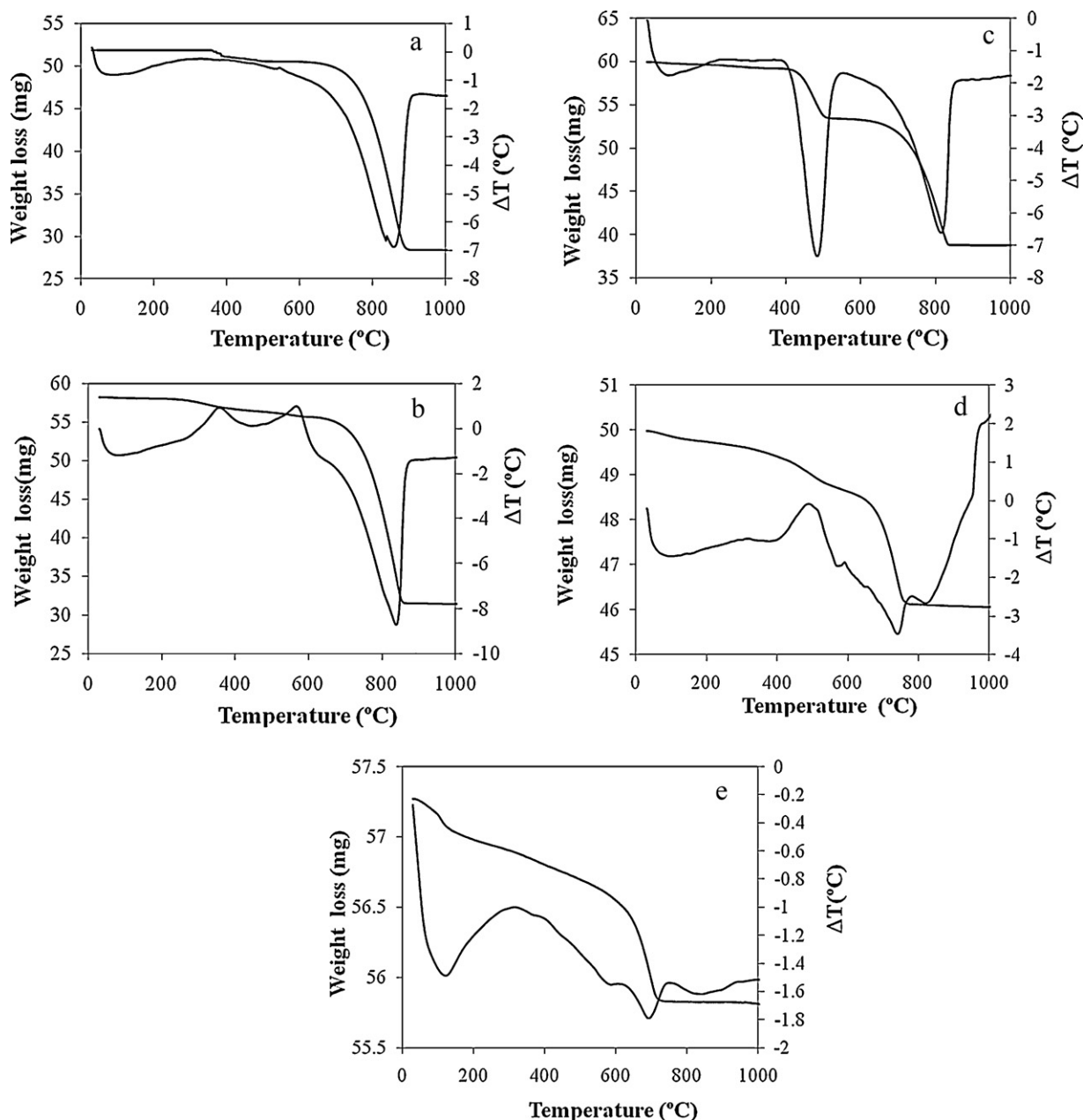


Fig. 2. TGA–DTA of (a) marble, (b) mussel, (c) commercial calcium hydroxide, (d) biomass ash, and (e) chamotte.

portlandite ( $\text{Ca}(\text{OH})_2$ ) formed by the moistening of the  $\text{CaO}$ . It showed an endothermic peak centred around  $473^\circ\text{C}$ . The last and most intense weight loss of 27.5% occurred from  $473^\circ\text{C}$  to  $850^\circ\text{C}$ , due to the decomposition of the calcite ( $\text{CaCO}_3$ ), with a strong endothermic peak centred around  $802^\circ\text{C}$ .

The TGA–DTA curve of the biomass ash residue (Fig. 2d) showed an endothermic peak at approximately  $87^\circ\text{C}$  with a weight loss of 0.4%, corresponding to the elimination of the moisture in the ashes. From 160 to  $390^\circ\text{C}$ , a slight exothermic peak due to the elimination of organic material present in the ashes was observed, producing a weight loss of 0.7%. From  $390^\circ\text{C}$  to  $560^\circ\text{C}$ , the combustion of the unburned elements in the ashes occurred, giving a weight loss of 1.4%, with an exothermic peak centred around  $480^\circ\text{C}$ . From  $560^\circ\text{C}$  to  $830^\circ\text{C}$ , the greatest weight loss occurred (5.4%), showing

various thermal effects. At  $730^\circ\text{C}$ , an endothermic peak due to the elimination of structural water from the hydroxide ions present in the residue was observed. The exothermic peak at  $770^\circ\text{C}$  was probably due to more combustion reactions of the unburned elements present in the ashes, whereas the endothermic effect at  $815^\circ\text{C}$  may be due to the decomposition of the carbonates in the ashes.

The TGA–DTA of the chamotte residue (Fig. 2f) showed a small weight loss of 0.4%, from ambient temperature up to  $130^\circ\text{C}$ , due to water loss, showing an endothermic peak centred around  $115^\circ\text{C}$ . The mass loss continued until  $500^\circ\text{C}$  (0.6%) due to the oxidation of the organic matter (exothermic peak centred around  $314^\circ\text{C}$ ). From  $500^\circ\text{C}$  to  $735^\circ\text{C}$ , the greatest mass loss, of 1.5% was observed due to the dehydration of the ferrous and aluminium oxides (endothermic peak centred around



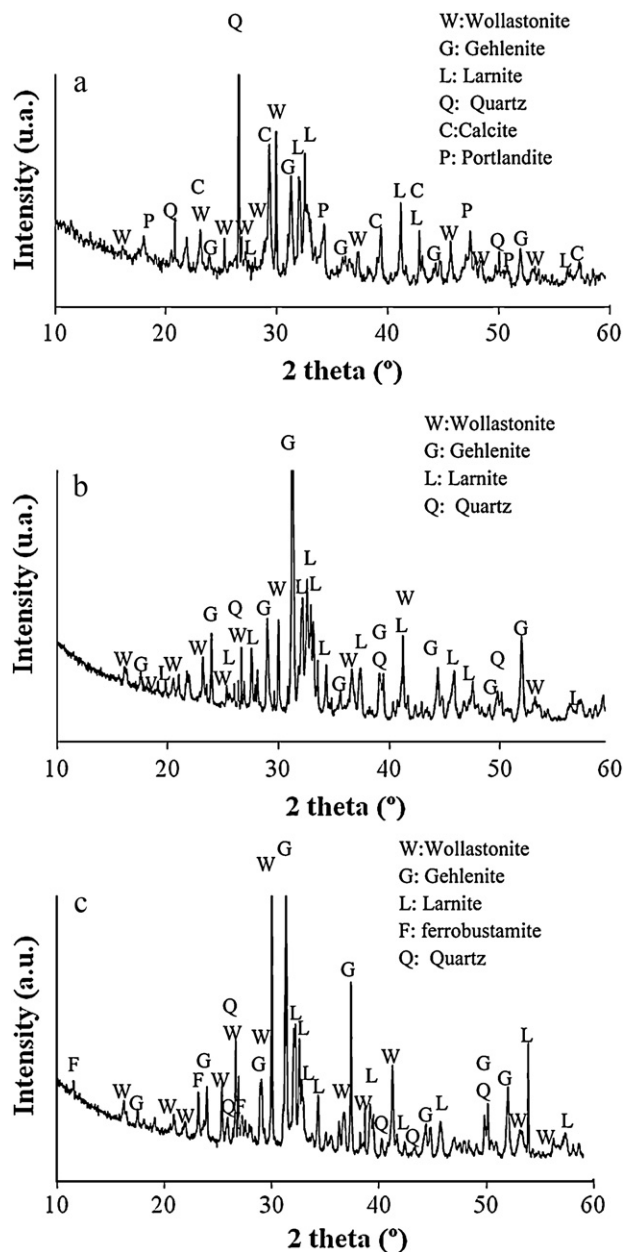


Fig. 3. XRD patterns of silicate obtained using as raw materials (a) marble and biomass ash, (b) mussel and biomass ash, and (c) commercial calcium hydroxide and chamotte.

685 °C), as well as the presence of quartz and dehydration due to the breaking of the crystal lattice of silicates (endothermic peak centred around 743 °C). Finally, the small endothermic peak centred around 842 °C may be due to the decomposition of the carbonates at 750–800 °C, involving a very small weight loss.

The materials obtained after mixing the reagents of biomass ash and marble, biomass ash and commercial calcium hydroxide, and ceramic residue (chamotte) and mussel shells in a molar ratio  $\text{SiO}_2\text{:CaO}$  1:1 and subsequently sintering them at 1100 °C were characterized using XRD and TGA–DTA.

The XRD data of the materials obtained after mixing and sintering the reagents indicated that the sintering produced not only wollastonite ( $\text{CaSiO}_3$ ), as indicated in the phase diagram

$\text{SiO}_2\text{--CaO}$  but also silicates such as gehlenite ( $\text{Ca}_2\text{Al}(\text{AlSi})\text{O}_7$ ) and larnite ( $\text{Ca}_2\text{SiO}_4$ ) (Fig. 3). In the synthesis that uses reagents of chamotte and mussel dust (Fig. 3b), small quantities of ferrobustamite ( $(\text{Ca,Fe,Mn})_3\text{Si}_3\text{O}_9$ ) were also observed. In addition, in the sintering that used ashes and marble as raw materials (Fig. 3a), sharp diffraction peaks of the raw materials that had not reacted completely were observed, such as calcite ( $\text{CaCO}_3$ ), quartz ( $\text{SiO}_2$ ) and portlandite ( $\text{Ca}(\text{OH})_2$ ). In the other two sintering processes, the diffraction peak for quartz ( $\text{SiO}_2$ ) was only observed. However, the proportion of silicates formed was different. When raw materials of ash and marble or chamotte and mussel powder were used, gehlenite and wollastonite formed in similar proportions with greater yield from the second reaction. When biomass ash and commercial calcium hydroxide were employed (Fig. 3c), the predominant silicate was gehlenite, along with a smaller quantity of wollastonite, as indicated by the diffraction peaks. The presence of impurities in the form of alkaline, ferrous, magnesium and aluminium oxides not only encourages the formation of liquid phase at a lower temperature (1100 °C) than that shown in the phase diagram  $\text{CaO--SiO}_2$  (1450 °C) [23] but also encourages the formation of wollastonite [24] when the impurities are found at less than 3.6%. All of the residues contained impurities. The percentage of mineralizers was greater, however, when chamotte and mussel shell were used than when biomass ash and marble or commercial calcium hydroxide were used. Therefore, the formation of wollastonite is encouraged when raw materials like chamotte and mussel were used in synthesis.

TGA curves of the synthesized samples (Fig. 4) showed a total weight loss of about 7 wt% for sintered samples using biomass ash residue and marble or chamotte and mussel shells as raw materials, while the sintered sample using biomass ash and commercial calcium hydroxide showed a lower total weight loss of only 3%. In the TGA–DTA of the silicates obtained using biomass ash residues and marble, Fig. 4a showed a small endothermic peak at 120 °C, which could be attributed to physically adsorbed water loss, giving an approximate weight loss of 0.5%. At temperatures from 380 to 490 °C, oxidation reactions occurred in the organic material, as can be seen in the moderate but continuous mass loss (0.8%), which produced an exothermic effect. At 420 °C, a strong endothermic effect corresponding to the dehydration of portlandite, unreacted quartz  $\alpha \rightarrow \beta$  transformation and dehydroxilation due to the breaking of the crystal lattice of the silicates formed was observed. Finally, at 750 °C, a strong endothermic effect due to the thermal decomposition of the unreacted  $\text{CaCO}_3$  (calcite) into  $\text{CaO} + \text{CO}_2$  was observed, with a weight loss of 5.2%.

In the TGA–DTA of the samples synthesized using biomass ash and commercial calcium hydroxide as raw materials (Fig. 4b), a small weight loss in two stages was observed. These stages corresponded to the loss of the physically absorbed water. Two endothermic effects centred around 110 °C and 200 °C were showed, which may be due to the fact that the ashes used as raw material had a larger particle size, which may change the extent of the peak. From 250 °C to 485 °C, the slight

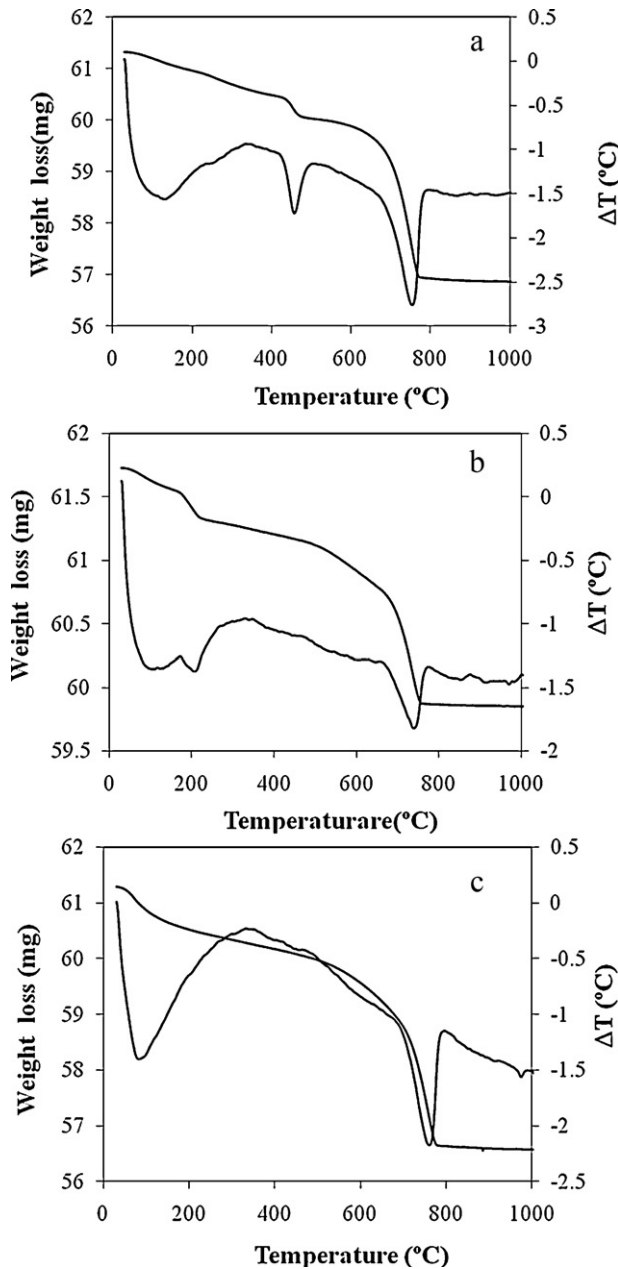


Fig. 4. TGA–DTA of silicate obtained using as raw materials (a) marble and biomass ash, (b) mussel and biomass ash, and (c) commercial calcium hydroxide and chamotte.

weight loss continues (0.3%) due to the combustion of the organic material, showing an exothermic effect at 300 °C. The weight loss continued until 780 °C (2.1%) and could be attributed to the allotropic change of unreacted quartz and dehydration due to breaking of the crystal lattice in the silicates

formed, showing an endothermic effect at 730 °C. The same tendency was observed in the TGA–DTA of the sintered samples using chamotte and mussel shells as raw material (Fig. 4c), showing an endothermic effect at 75 °C due to water loss. The weight loss of 1.1% from 150 °C to 500 °C was due to the combustion of the organic material (exothermic at 330 °C). The greatest weight loss of 5.6% from 500 °C to 840 °C was attributed to the unreacted quartz  $\alpha \rightarrow \beta$  allotropic transformation and dehydroxilation of the silicates formed showing an endothermic effect at 750 °C. DTA curves of three samples showed after about 850 °C an exothermic effect without a mass change due to the crystallization of silicates formed.

To determine whether the sintered materials could be used as thermal insulating ceramics, the silicates synthesized were compressed. The absolute density of all of the samples was similar, yielding values close to 2000 kg/m<sup>3</sup>. The data on bulk density were similar, yielding a lower value, 1700 kg/m<sup>3</sup>, for the sintered samples using biomass ash and commercial calcium hydroxide (Table 2). Thus, these samples showed a greater value for total porosity. There was no correlation between the organic material content of the residues used and the porosity, since the content of organic material determined by the CNH analysis of the mixture of biomass ash and marble (8.1%) and the mussel shell-chamotte mix (6.9%) was greater than the content of organic material in the mixture of ashes and commercial calcium hydroxide (3.1%). The data indicated that both the organic material and the calcium carbonate present in the samples contributed to the formation of porosity.

The total porosity of the samples may be of two kinds, open and closed. Open porosity can be determined from the values of water absorption. The lower the water absorption, the greater the expected durability and resistance to external climatological conditions. The data for water absorption (Fig. 5) indicated that the sintered samples that used the biomass ash and commercial calcium hydroxide as reagents and the samples using chamotte and mussel showed greater values of absorption and thus greater open porosity. According to the XRD pattern of these samples, all of the CaCO<sub>3</sub> reacted, giving rise to CaO. The CaO then reacted to form silicates, creating the possibility of open porosity, since these samples contained less organic material. In contrast, in the samples that contained biomass ash and marble as reagent, not all of the CaCO<sub>3</sub> reacted. This was demonstrated by their XRD pattern, which showed lower values for water absorption despite the greater value for organic material.

Water suction is the amount of water than can rise due to capillary action in a piece. This property affects the quality of the final material and its durability significantly. High values should be avoided, since they can cause pieces with defects and

Table 2

Bulk density, absolute density and water suction of the specimens prepared by mixing and sintering at 1100° C using different waste SiO<sub>2</sub>/CaO = 1:1 molar ratio.

Sample	Bulk density (g/cm <sup>3</sup> )	Absolute density (kg/m <sup>3</sup> )	Water suction (kg/m <sup>2</sup> min)	Thermal conductivity (W/m K)
Ash–marble	2.05 ± 0.04	2120 ± 51	0.02 ± 0.01	0.18
Ash–CaO	1.70 ± 0.01	1970 ± 32	2.20 ± 0.11	0.10
Chamotte–mussel	1.95 ± 0.02	2030 ± 71	0.38 ± 0.07	0.12

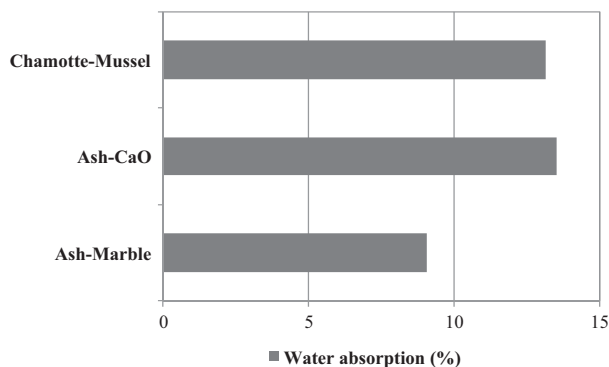


Fig. 5. Water absorption of bricks.

lower durability. According to the UNE standard, water suction should be less than  $4.5 \text{ kg/m}^2 \text{ min}$ . The samples that used biomass ash and commercial calcium hydroxide ( $2.2 \text{ kg/m}^2 \text{ min}$ ) show much higher water suction values than those that used marble as a source of calcium and suction values almost six times higher than those that used chamotte as a source of silica or mussel as a source of calcium oxide ( $0.4 \text{ kg/m}^2 \text{ min}$ ) (Table 2). Therefore, after the sintering process and shaping, the mix of biomass ash and commercial calcium hydroxide produced samples with greater interconnected surface porosity. However, all of the samples met the UNE standard.

Compressive strength in ceramic materials is the most important index of engineering quality for construction materials. According to the UNE standard, the compressive strength of the bricks should be at least 10 MPa. The synthesized samples of the biomass ash and commercial calcium hydroxide showed the lowest value for compressive strength (29.8 MPa) (Fig. 6). This was due to the fact that the material showed greater open porosity and much greater interconnected surface porosity, as indicated by the data for water absorption and water suction, respectively. Interconnected porosity could act as a centre for accumulation of tensions, permitting the propagation of cracks. In contrast, the samples synthesized using biomass ash and marble presented a higher value of compressive strength (59.3 MPa). Although their total porosity was similar to that of the other samples, their open porosity and especially their interconnected surface porosity were much lower. In all of the cases, compressive

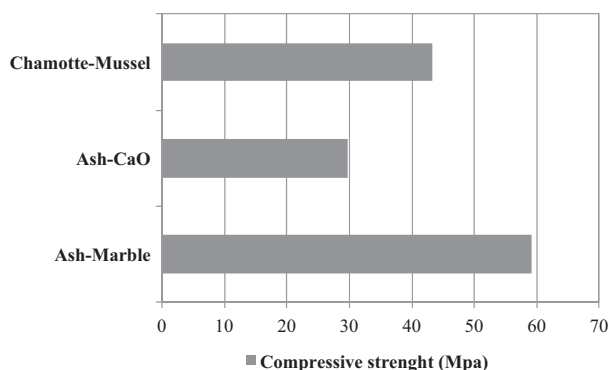


Fig. 6. Compressive strength of bricks.

strength achieved values much higher than those required by the UNE standard. The samples were thus apt for structural enclosures.

To determine the applicability of the formed materials as low temperature thermally insulating ceramic the thermal conductivity were determined. The values for thermal conductivity obtained corresponded to insulating materials. In all cases, they were lower than the reference value of  $0.43 \text{ W/mK}$  established by the UNE-EN 1745 standard [25]. This property varied from  $0.10 \text{ W/mK}$  for the samples sintered by solid state reaction between biomass ash and commercial calcium hydroxide to  $0.18 \text{ W/mK}$  for the samples sintered by the reaction of biomass ash and marble. There was no linear relation between the bulk density, which gives us the total porosity and the conductivity. Therefore, the data indicate that the thermal conductivity of the pieces did not depend only on the total porosity but also on the kind of porosity of the pieces (open vs. closed) and the pore size.

A linear relationship between water absorption (indirect measure of open porosity) and thermal conductivity (Fig. 7) was observed. The data fit a straight line with negative slope, which indicates that the increase in open porosity in the pieces decreases their conductivity. According to Avgustinik [26], closed porosity is the cause of thermal insulation in materials. Large pores cause an increase in thermal conductivity, and finer and more uniform pores lead to a greater capacity for thermal insulation. The samples synthesized by solid state reaction between biomass ash and commercial calcium hydroxide showed greater total porosity, greater open porosity, and greater interconnected surface porosity and thus a smaller quantity of closed porosity. These samples must contain finer, more uniform pores than the samples sintered by mixing reagents using the same source of silica, biomass ash and marble. In spite of having greater closed porosity, the latter have higher thermal conductivity. Therefore, the pores in this sample were large, causing a decrease in the insulating capacity.

The morphological analysis of the sintered samples was determined by a scanning electron microscope (SEM) connected to an energy dispersive X-ray microanalyzer (EDAX) to determine the ratio of the constitutive all of the micrographs, the presence of calcium silicate particles composed mostly of  $\text{CaO}$  and  $\text{SiO}_2$  were observed. The EDAX

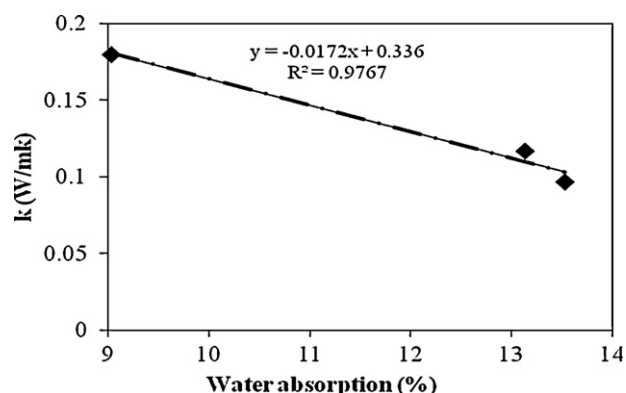


Fig. 7. Thermal conductivity vs. absorption water of bricks.



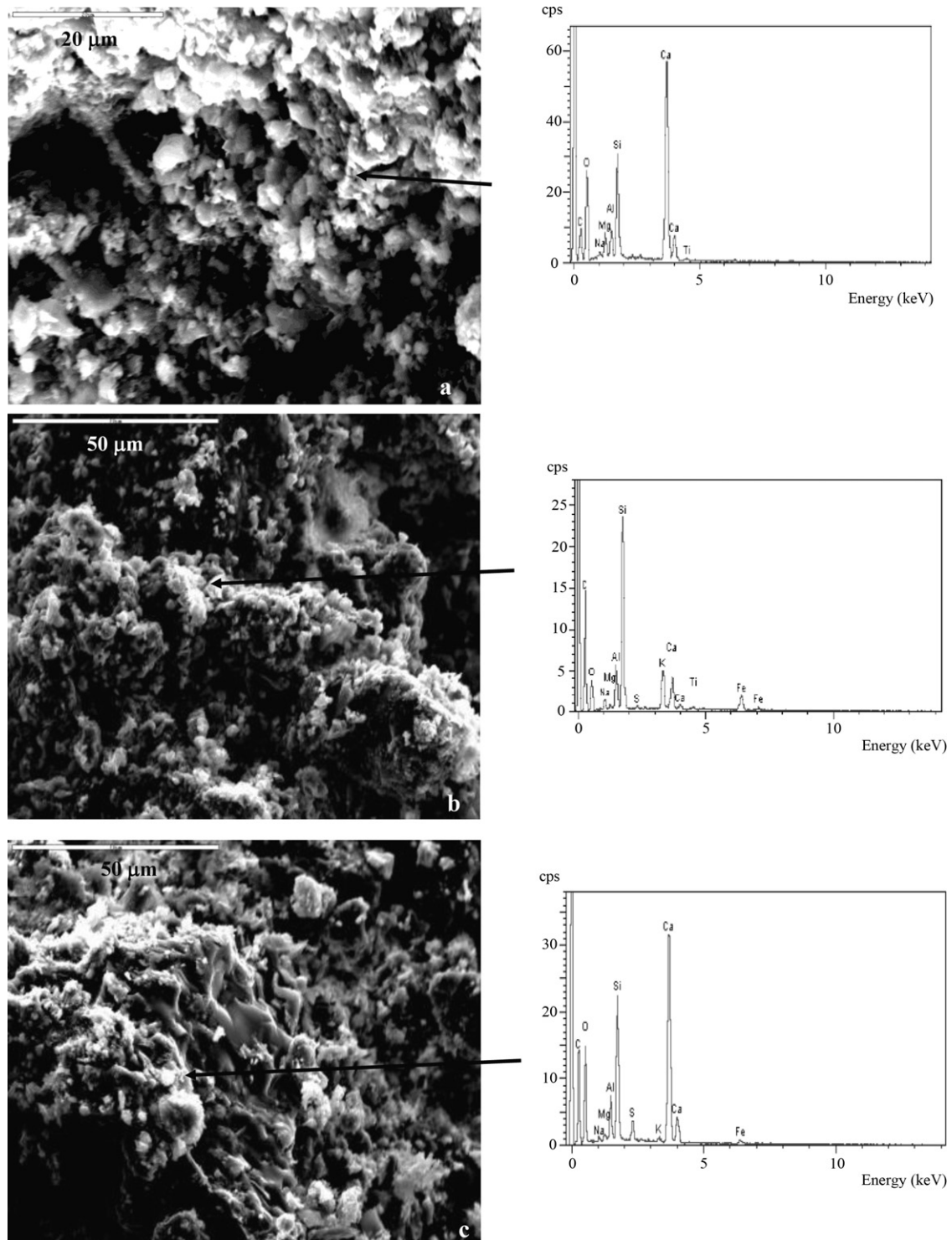


Fig. 8. SEM micrographs of silicate obtained using as raw materials (a) marble and biomass ash, (b) mussel and biomass ash, and (c) commercial calcium hydroxide and chamotte.

analysis (Fig. 8) showed that also contained other components, such as  $\text{Al}_2\text{O}_3$ ,  $\text{MgO}$ , and  $\text{NaO}$ , as well as  $\text{Fe}_2\text{O}_3$  and  $\text{TiO}_2$ . All of the samples showed porosity. Open porosity was higher in the samples sintered by solid state reaction of biomass ash and calcium hydroxide but lower in the samples sintered by mixing biomass ash and marble, according to the water absorption data. In addition, the samples showed the presence of closed porosity,

although the pore size is different. The samples obtained by reaction of biomass ash and marble showed a greater pore size.

#### 4. Conclusions

It is possible to obtain calcium silicates for use as low temperature thermally insulating materials from different

residues. The use of residues is an interesting and profitable alternative from both the economic and the environmental perspective. Using valued residues as raw materials minimizes the expense and effects of depositing them in dumps. The main calcium silicates obtained were gehlenite, larnite, and wollastonite, although the proportion of each of these depended on the reagents used as raw materials. The silicates synthesized and formed for use as construction material presented values of bulk density between 1700 and 2100 kg/m<sup>3</sup>. The samples synthesized using biomass ash and commercial calcium hydroxide as reagents had less bulk density and lower values for thermal conductivity, providing better thermal insulation, but their resistance to compression was lower. From the results obtained, it could conclude that the conductivity values depend on both the kind of porosity and the pore size. The samples synthesized using biomass ash and commercial calcium hydroxide showed a greater value of open porosity and interconnected surface porosity. These samples also had a smaller pore size, as the SEM study indicated. All of the synthesized materials met the UNE standard for use as low temperature insulating construction materials, which can contribute to considerable energy savings in the buildings constructed from these materials.

## References

- [1] M. Dondi, M. Marsigli, B. Fabri, Recycling of urban and industrial wastes in brick production: a review, *Tile Brick Int.* 13 (1997) 302–315.
- [2] M. Dondi, M. Marsigli, B. Fabbri, Recycling of industrial and urban wastes in brick production: a review, *Tile Brick Int.* 13 (1997) 218–225.
- [3] J.M.F. Ferreira, P.J. Guedes, P. Torres, R.S. Manjate, H.R. Fernandes, Recycling of industrial wastes—an overview about successful case studies, in: Pecchio, et al. (Eds.), *Applied Mineralogy*, ICAM-BR, São Paulo, 2004, p. 33.
- [4] W.T. Tsai, Y.H. Chou, A review of environmental and economic regulations for promoting industrial waste recycling in Taiwan, *Waste Manage.* 24 (2004) 1061–1069.
- [5] A. Pappu, M. Saxena, S.R. Asolekar, Solid wastes generation in India and their recycling potential in building materials, *Build. Environ.* 42 (2007) 2311–2320.
- [6] HISPALYT, Asociación Española de Fabricantes de Ladrillos y Tejas de Arcilla Cocida, 2007.
- [7] P. Kittl, G. Diaz, H. Alarcón, Dosification of a cement-talc-chamotte refractory mortar subjected to thermal shock, *Cement Concrete Res.* 22 (1992) 736–742.
- [8] A. Capoglu, P.F. Messer, Design and development of a chamotte for use in a low-clay translucent whiteware, *J. Eur. Ceram. Soc.* 24 (2004) 2067–2072.
- [9] C.M.F. Vieira, S.N. Monteiro, Effect of grog addition on the properties and microstructure of a red ceramic body for brick production, *Constr. Build. Mater.* 21 (2007) 1754–1759.
- [10] C.N. Djangang, A. Elimbi, U.C. Melo, G.L. Lecomte, C. Nkoumbou, J. Soro, J.P. Bonnet, P. Blanchart, D. Njopwouo, Sintering of clay-chamotte ceramic composites for refractory bricks, *Ceram. Int.* 34 (2008) 1207–1213.
- [11] F. Puertas, I. García-Díaz, A. Barba, M.F. Gazulla, M. Palacios, M.P. Gómez, S. Martínez-Ramírez, Ceramic wastes as alternative raw materials for Portland cement clinker production, *Cement Concrete Comp.* 30 (2008) 798–805.
- [12] J.R. Taylor, A.T. Didsdale, Thermodynamic and phase diagram data for the CaO–SiO<sub>2</sub> system, *Calphad* 14 (1996) 71–88.
- [13] E.M. Levin, C.R. Robbins, H.F. McMurdie, Phase diagrams for ceramists, *Am. Ceram. Soc.* (1996), Fig. 237.
- [14] L.L. Hench, Bioceramic from concept to clinic, *J. Am. Ceram. Soc.* 74 (1991) 1487–1510.
- [15] P.N. de Aza, A.H. de Aza, S. de Aza, Crystalline bioceramic materials, *Bol. Soc. Esp. Ceram. Vidrio* 44 (2005) 135–145.
- [16] L.L. Long, L.D. Chen, J. Chang, Low temperature fabrication and characterization of  $\beta$ -CaSiO<sub>3</sub> ceramics, *Ceram. Int.* 33 (2006) 457–460.
- [17] J.H. Johnston, T. Borrmann, D. Rankin, M. Cairns, J.E. Grindrod, A. Mcfarlane, Nano-structured composite calcium silicate and some novel applications, *Curr. Appl. Phys.* 8 (2008) 504–507.
- [18] M.G. Gandolfi, G. Ciapetti, P. Taddei, F. Perut, A. Tinti, M.V. Cardoso, B. Van Meerbeek, C. Prati, Apatite formation on bioactive calcium–silicate cements for dentistry affects surface topography and human marrow stromal cells proliferation, *Dent. Mater.* 26 (2010) 974–992.
- [19] UNE EN 772-13: 2001, Methods of Test for Masonry Units—Part 13: Determination of Net and Gross Dry Density of Masonry Units (except for natural stone).
- [20] UNE 67027: 1984, Burned Clay Bricks. Determination of the Water Absorption.
- [21] UNE 67031: 1986, Burned Clay Bricks. Suction Test.
- [22] UNE EN 772-1:2002, Methods of Test for Masonry Units—Part 1: Determination of Compressive Strength.
- [23] B. Philip, A. Muan, Phase diagram of CaO–SiO<sub>2</sub>, *J. Am. Ceram. Soc.* (1959) 414.
- [24] I. Kotsis, A. Balogh, Synthesis of wollastonite, *Ceram. Int.* 15 (1989) 79–85.
- [25] UNE-EN 1745:2002, Masonry and Masonry Products—Methods for Determining Desing Thermal Values.
- [26] A.I. Avgustinik, 2nd ed., *Cerámica*, Reverté, S.A., Barcelona, 1983.